Dual Purpose Bridge Health Monitoring and Weigh-in-motion (BWIM) Phase I

FINAL REPORT

Richard Christenson and Sarira Motaref

Report Number

CT-2265-F-15-7

SPR-2265

Submitted to the

Connecticut Department of Transportation
Bureau of Policy and Planning
Roadway Information Systems Research Section

Michael Connors
Assistant Planning Director

July 7, 2016

Department of Civil and Environmental Engineering
School of Engineering
University of Connecticut

Disclaimer

This report [article, paper or publication] does not constitute a standard, specification or regulation. The contents of this report reflect the views of the authors who are responsible for the facts and the accuracy of the data presented herein. The contents do not necessarily reflect the views of the Connecticut Department of Transportation or the Federal Highway Administration.

Acknowledgments

The authors would like to acknowledge the efforts of numerous Connecticut Department of Transportation employees in particular Anne-Marie McDonnell and Paul Dattilio. The authors would also like to acknowledge the efforts of Susan Bakulski who worked as a research assistant at the University of Connecticut on this project.

This report was prepared by the University of Connecticut, in cooperation with the Connecticut Department of Transportation and the United States Department of Transportation, Federal Highway Administration. The opinions, findings and conclusions expressed in the publication are those of the authors and not necessarily those of the Connecticut Department of Transportation or the Federal Highway Administration.

SI* (MODERN METRIC) CONVERSION FACTORS

APPROXIMATE CONVERSIONS TO SI UNITS

Symbol	When You Know	Multiply By	To Find	Symbol
		LENGTH		
in	inches	25.4	millimeters	mm
ft	feet	0.305	meters	m
yd	yards	0.914	meters	m
mi	miles	1.61	kilometers	km
		AREA		
in^2	square inches	645.2	square millimeters	mm^2
ft^2	square feet	0.093	square meters	m^2
yd^2	square yard	0.836	square meters	m^2
ac	acres	0.405	hectares	ha
mi^2	square miles	2.59	square kilometers	km^2
		VOLUME		
fl oz	fluid ounces	29.57	milliliters	mL
gal	gallons	3.785	liters	L
ft^3	cubic feet	0.028	cubic meters	m^3
yd^3	cubic yards	0.765	cubic meters	m^3
	NOTE: volumes greater than 1000 L shall be shown in m^3			
		MASS		
oz	ounces	28.35	grams	g
lb	pounds	0.454	kilograms	kg
T	short tons (2000 lb)	0.907	megagrams (or "metric ton")	Mg (or "t")
		TEMPERATURE (exact degrees)		
^oF	Fahrenheit	5 (F-32)/9 or (F-32)/1.8	Celsius	^oC
		ILLUMINATION		
fc	foot-candles	10.76	lux	lx
fl	foot-Lamberts	3.426	$candela/m^2$	cd/m^2
		FORCE and PRESSURE or STRESS		
lbf	poundforce	4.45	newtons	N
lbf/in^2	poundforce per square inch	6.89	kilopascals	kPa

APPROXIMATE CONVERSIONS FROM SI UNITS

Symbol	When You Know	Multiply By	To Find	Symbol
		LENGTH		
mm	millimeters	0.039	inches	in
m	meters	3.28	feet	ft
m	meters	1.09	yards	yd
km	kilometers	0.621	miles	mi
		AREA		
mm^2	square millimeters	0.0016	square inches	in^2
m^2	square meters	10.764	square feet	ft^2
m^2	square meters	1.195	square yards	yd^2
ha	hectares	2.47	acres	ac
km^2	square kilometers	0.386	square miles	mi^2
		VOLUME		
mL	milliliters	0.034	fluid ounces	fl oz
L	liters	0.264	gallons	gal
m^3	cubic meters	35.314	cubic feet	ft^3
m^3	cubic meters	1.307	cubic yards	yd^3
		MASS		
g	grams	0.035	ounces	oz
kg	kilograms	2.202	pounds	lb
Mg (or "t")	megagrams (or "metric ton")	1.103	short tons (2000 lb)	T
		TEMPERATURE (exact degrees)		
^oC	Celsius	1.8C+32	Fahrenheit	^oF
		ILLUMINATION		
lx	lux	0.0929	foot-candles	fc
cd/m^2	$candela/m^2$	0.2919	foot-Lamberts	fl
		FORCE and PRESSURE or STRESS		
N	newtons	0.225	poundforce	lbf
kPa	kilopascals	0.145	poundforce per square inch	lbf/in^2

*SI is the symbol for the International System of Units. Appropriate rounding should be made to comply with Section 4 of ASTM E380.
(Revised March 2003)

Technical Report Documentation Page

1. Report No. CT-2265-F-15-7	2. Government Accession No.	3. Recipient's Catalog No.
4. Title and Subtitle Dual Purpose Bridge Health Monitoring and Weigh-in-motion (BWIM) - Phase I		5. Report Date July 7, 2016 6. Performing Organization Code
7. Author(s) Richard Christenson and Sarira Motaref		8. Performing Organization Report No.
9. Performing Organization Name and Address University of Connecticut Connecticut Transportation Institute 270 Middle Turnpike, U-5202 Storrs, Connecticut 06269-5202		10 Work Unit No. (TRIS) N/A 11. Contract or Grant No. N/A 13. Type of Report and Period Covered Final Report August 1, 2009 – June 30, 2011
12. Sponsoring Agency Name and Address Connecticut Department of Transportation 2800 Berlin Turnpike Newington, CT 06131-7546		14. Sponsoring Agency Code SPR-2265
15. Supplementary Notes Prepared in cooperation with the U.S. Department of Transportation, Federal Highway Administration, Connecticut Department of Transportation		

16. Abstract

The dual-purpose bridge health monitoring (BHM) and bridge weigh-in-motion (BWIM) system proposed in this research project establishes a single monitoring system, comprised of sensors, data acquisition, and processing, to provide both long-term health monitoring of a highway bridge and bridge-weigh-in-motion capabilities. A prototype dual-purpose BHM/BWIM system is presented that has been designed to examine the challenges associated with implementing a combined BHM/BWIM bridge monitoring system. This prototype system is currently being deployed in Connecticut on Interstate 91 (I-91) northbound in the town of Meriden, Connecticut. The BHM/BWIM design and initial results are provided in this report.

17. Key Words Bridge Monitoring, Weigh-in-motion, BWIM, Bridge Structural Health, Bridge Inspection, Vibration Sensors	18. Distribution Statement No restrictions. This document is available to the public through the National Technical Information Service, Springfield, Virginia 22161. The report is available on-line from National Transportation Library at http://ntl.bts.gov.

19. Security Classif. (of report) Unclassified	20. Security Classif. (of this page) Unclassified	21. No. of Pages 58	21. Price
Form DOT F 1700.7 (8-72)	Reproduction of completed page authorized		

Table of Contents

List of Tables

List of Figures

Executive Summary

The dual-purpose bridge health monitoring (BHM) and bridge weigh-in-motion (BWIM) system proposed in this research project establishes a single monitoring system, comprised of sensors, data acquisition, and processing, to provide both long-term health monitoring of a highway bridge and bridge-weigh-in-motion capabilities. A prototype dual-purpose BHM/BWIM system is presented that has been designed to examine the challenges associated with implementing a combined BHM/BWIM bridge monitoring system. This prototype system is currently being deployed in Connecticut on Interstate 91 (I-91) northbound in the town of Meriden, Connecticut. The BHM/BWIM design and initial results are provided in this report.

1-INTRODUCTION

The dual-purpose bridge health monitoring and weigh-in-motion system proposed in this research project establishes a single monitoring system, comprised of sensors, data acquisition, and processing, to provide both long-term health monitoring of a highway bridge and bridge-weigh-in-motion capabilities. The goal of long-term bridge monitoring is to identify changes in a bridge's dynamic behavior over multi-year periods as an indicator of the structural health of the bridge. To achieve this goal, highway bridges are instrumented with sensors, data acquisition and processing power. Vibration-based health monitoring shows great promise to supplement bridge inspections and provide bridge owners with timely information on the structural condition of the bridge infrastructure. The premise of vibration-based monitoring is that damage or a change in the structure will result in a corresponding change in the stiffness (or mass) of the structure, which will change the structure's dynamic characteristics and ultimately the response to a dynamic loading.

Transportation agencies are faced with the need to design and improve transportation networks to meet the ever increasing demand for safe, efficient and cost effective transport of people and goods. To meet this need, whether for the design of infrastructure (bridges and pavements), application of air quality or freight models, or enforcement of the size and weight limits, information is needed to quantify the loads experienced on the network. Weight data and related traffic data are used for a variety of engineering designs and decisions. Weigh-in-motion (WIM) systems are one mechanism used to gather such weight data. WIM systems present many challenges to employ,

including cost, installation, calibration, maintenance and accuracy. Alternative means to collect weight data, in particular non-intrusive methods, are desired.

Bridge Weigh-In-Motion (BWIM) uses the dynamic response of a bridge to determine gross weight, speed, and axle spacing of vehicles. The advantage of BWIM is that it does not require installation of sensors in the pavement, nor use any axle detectors in the roadway. To date, studies have all been short-term applications of BWIM. A recent study by the Connecticut Academy of Science and Engineering (CASE) recommends that BWIM, as a promising non-intrusive technology, should be considered for WIM in Connecticut (CASE, 2008).

Bridge WIM systems and bridge health monitoring (BHM) systems, which use structural response measurements to identify the structural condition of the bridge, have similar components. By considering this leveraged BHM/BWIM application, more comprehensive data can be collected. Augmenting long-term bridge monitoring systems with BWIM will enable agencies to collect weight data on a more comprehensive network. Improved load information on the transportation network will lead to better bridge, pavement and highway designs, as well as improved decisions and efficiency; the ability to weigh and screen commercial vehicles in a timely fashion for weight enforcement; the collection of speed, weight and class data for traffic monitoring; and increased safety and timely identification of changes in the structural system for maintenance and operation. The actual measured volume and speed of traffic combined with indicators of structural degradation can also benefit planning, if implemented at a system level. Truck traffic attributes that are important for weight enforcement,

structural health monitoring, and traffic monitoring can be determined and shared through the use of combined BHM/BWIM systems.

A prototype dual-purpose BHM/BWIM system is presented that has been designed to examine the challenges associated with implementing a combined BHM/BWIM bridge monitoring system. This prototype system is currently being deployed in Connecticut on Interstate 91 (I-91) northbound in the town of Meriden, Connecticut. The bridge is ideally located prior to an operational Connecticut static weigh scale. This proximity will not only allow the project to validate BWIM measurements with the static scale, but will facilitate assessment of how the results from a leveraged BHM/BWIM system can benefit enforcement, bridge health monitoring and traffic monitoring efforts at federal, state and local transportation agencies.

Figure 1: Installation of the dual BHM/BWIM system on the Meriden Bridge.

The test bridge is a simply-supported steel-girder bridge built in 1964 located on I-91 over Baldwin Avenue in Meriden, Connecticut, and referred to herein as the Meriden Bridge. Figure 1 shows a picture of the Bridge during installation of the monitoring system. This single-span bridge is 85 feet in length with multiple plate-stringers supported by eight girders. The bridge has less than a 12% skew and 3% longitudinal slope. The bridge carries three lanes of Northbound traffic with an annual average daily traffic (AADT) of 57,000 vehicles, comprised of 9% trucks.

The physical equipment of the BWIM/BHM system includes instrumentation for an automatic data acquisition system to monitor dynamic beam strains and vertical acceleration due to traffic loading as well as the corresponding surface temperature of the bridge girders. Sensors measure physical responses (i.e. strain, acceleration and temperature) into analog electrical signals; and the data acquisition system converts the analog electrical signals of the sensors into digital signals. The output from the digital signals is saved for archiving and further processing purposes. It is possible to configure the system to compute real-time BHM and BWIM measurements, but for the purposes of this research the signals are saved for specific research objectives including the analysis of the sensor technologies for this application. Real-time computation of data in addition to saving the signals would require significantly more processing capabilities. The prototype BHM/BWIM system has been designed to meet specific research objectives including flexibility in available measurements for further BHM and BWIM development and evaluation of various sensor technologies for this application.

2-LITERATURE REVIEW

A brief literature review is provided in this section for both bridge weigh-in-motion and bridge health monitoring.

2-1- Bridge Weigh-In-Motion (BWIM)

Proposed over 30 years ago by Moses (Moses, 1979), BWIM continues to receive attention with the advancement of sensor and data acquisition technologies and with the extensive research conducted in Europe in the 1990's through the Weighing in motion of Axles and Vehicles for Europe (WAVE) project (Jacob, 2002). BWIM uses sensing, acquisition, and processing capabilities similar to those used in vibration-based BHM. Recent work on BWIM in France, Slovenia and Ireland has focused on fully portable temporary installations for enforcement and is typically limited to short single-span bridges. To date BWIM has been used in India, Canada and throughout Europe. A project to test and evaluate BWIM in the United States was recently conducted at the University of Alabama using the portable BWIM system developed in Europe. Additionally, the Connecticut Department of Transportation (CTDOT) and the University of Connecticut (UConn) have completed pilot studies on BWIM, in 2006 and 2008, which have focused on single-span steel-girder bridges (Cardini, A.J. and DeWolf, J.T. 2009; Wall C. and Christenson, R., 2009).

2-2- Bridge Health Monitoring (BHM)

Research is on-going in the area of long-term bridge monitoring, in particular long-term vibration-based monitoring for the purposes of detecting damage, monitoring deterioration and allocating resources (Farrar et al., 1999, Chakraborty et al., 1995, Salawu et al., 1997, Doebling et al., 1996, Caicedo et al., 2000, and Chang, 2000). Bridge Monitoring systems were specifically identified in the Federal SAFETEA-LU

Legislation [5202] (FHWA, 2005). The Connecticut Department of Transportation (CTDOT) and University of Connecticut (UConn) have a long history of close partnership in bridge monitoring, with over three decades of bridge health monitoring (BHM) experience. Connecticut has experience with six permanently monitored bridges that include a variety of bridge types including a post-tensioned segmental concrete box-girder, multi-girder steel composite, curved steel box-girder, hung span in a large truss, and continuous plate girder bridge (Olund et al., 2006, DeWolf et al., 2009, Scianna, et al., 2014a, 2014b, 2014c, and 2014d, Plude et al., 2014, Prusaczyk et al., 2014, and Christenson et al., 2014).

3-INSTRUMENTATION AND INSTALLATION

3.1 Sensors and Recording Tools

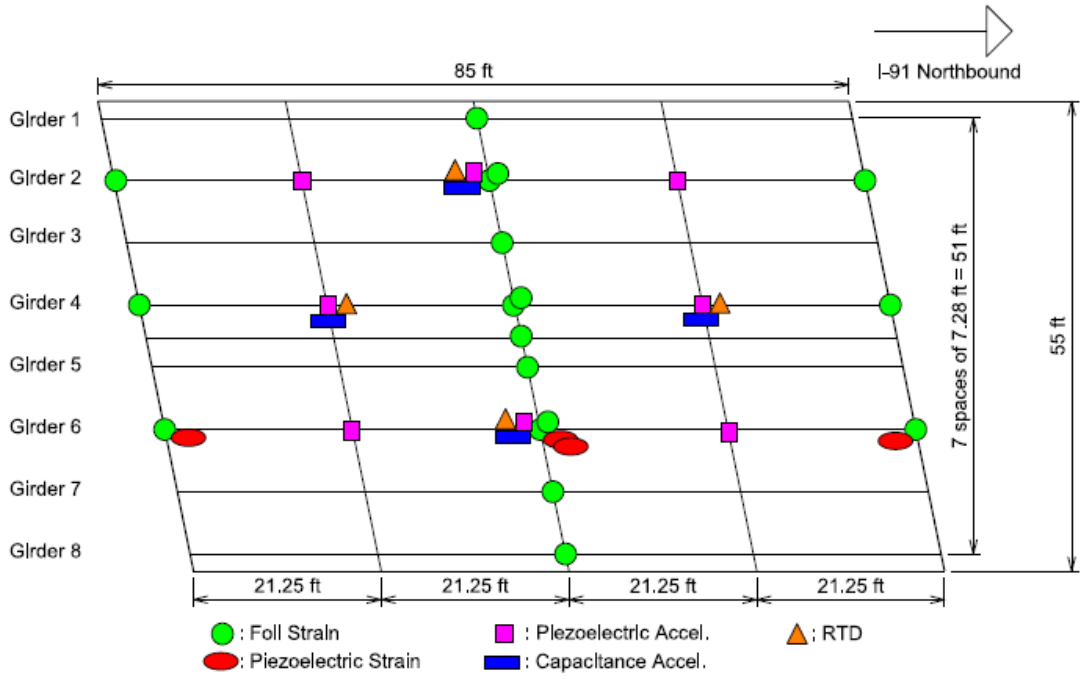

Figure 2: Schematic of sensors layout and sensors type for the Meriden Bridge

The Meriden Bridge has a dual-purpose BHM and BWIM system comprised of strain sensors, accelerometers, and temperature detectors for 38 total sensors and 5 different sensing technologies. There are eighteen foil strain gages, 4 piezoelectric strain sensors, 8 piezoelectric accelerometers, 4 capacitance accelerometers (with additional temperature sensing capability), and 4 resistance temperature detectors (RTD). The sensor layout and their types are shown in Figure 2.

3-1-1-Foil Strain Gages

Figure 3: Foil strain gages used on the Meriden Bridge

Foil strain sensors are commonly used for dynamic strain measurements in bridge monitoring. These sensors have a large measurement range, typically 1000s of microstrain (με). The bridge girders have been observed to have peak strains less than 100 με. Vishay Micro-Measurements manufactures the foil strain gages used for this installation.

A total of eighteen quarter-bridge foil-strain gages are installed on the Meriden Bridge. Figure 3 shows an image of the foil-strain gage prior to installation and Figure 4 provides a diagram of the sensor layout, as installed. Specifically:

- Six foil-strain sensors are installed on the bearings at bridge abutments on girders 2, 4, and 6. Bearings on girders 2, 4 and 6 were selected because each is located directly under one of the three lanes of traffic, respectively.

It is anticipated that the sensors installed at these locations will be well situated to detect vehicle loading on and off of the bridge and hence capture the presence of vehicles on the bridge.

- One foil strain gage is attached on the stringer in the middle of the bridge at the midspan (location K). This sensor is intended to measure axial strain in the stringer to identify if this stringer takes on any significant load during normal vehicle loading.
- Eleven foil strain gages are located at the midspan of steel girders 1 through 8 on the web, just above the bottom flange, and on girders 2, 4 and 6 on the web, just below the top flange. It is anticipated that the largest strain measurements will be collected at the midspan. The larger measurements provide a benefit of an improved signal-to-noise ratio. Having strain sensors on each of the eight girders enables the calculation of the strain distribution across the girders and also allows for strains resulting from vehicles traveling in multiple lanes across the bridge to be measured. Strain sensor measurements from the top and bottom of the web allow for the determination of the neutral axis for that particular cross-section. The location of the neutral axis is very important for bridge health monitoring. Applications of the neutral axis for BHM include: 1) the neutral axis is used in the assessment of the composite behavior of the bridge girders with respect to the bridge deck; 2) detection of any changes in the location of the neutral axis are indicative of deck damage.

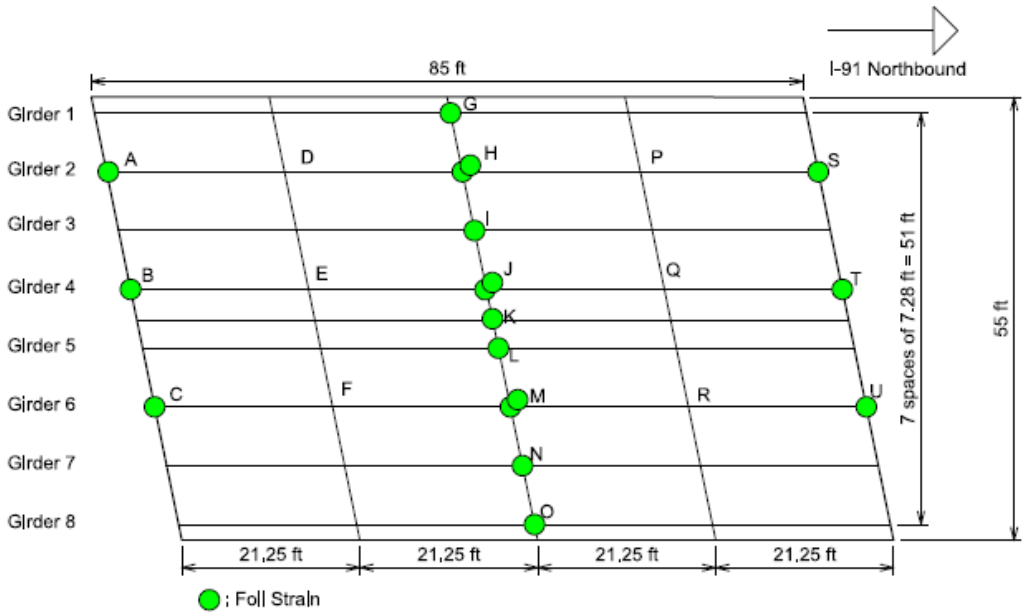

Figure 4: Foil Strain Sensor Layout (Plan View)

3-1-2-Piezoelectric Strain Gages

Figure 5: Piezoelectric strain sensors

Four piezoelectric strain gages, also referred to as high sensitivity quartz strain transducers, are installed on the Meriden Bridge (Fig. 5). All four sensors are located on girder 6. This girder was selected because it is directly below the right travel lane. The majority of the truck traffic travels in this right travel lane. There is one piezoelectric

strain gage at each bearing and two piezoelectric strain gages at the midspan, top and bottom of the web. These sensors are collocated with the foil strain gages. Figure 6 shows the piezoelectric strain sensors layout.

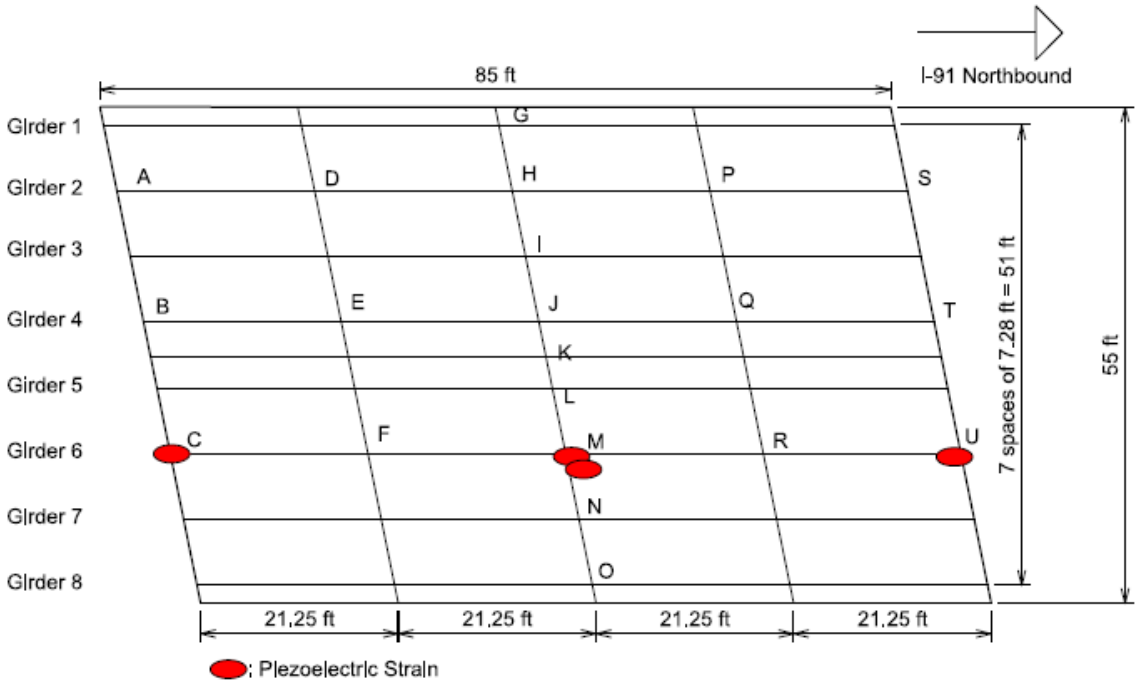

Figure 6: Plan view of piezoelectric strain sensors layout

The piezoelectric strain sensors can provide more sensitive strain measurements with a strain range of ±140 με and a bandwidth down to 0.004 Hz (a time constant of 113 seconds) for the configuration here. Use of this type of strain sensor to collect low frequency dynamic measurements on a highway bridge is a new application. The sensors are manufactured by the Kistler Instrument Corporation. Two additional components are used to convert the piezoelectric signal to a voltage output. They are the impedance converter (Model 558) and a range capacitor (Model 571A5), produced by National Instruments Corporation. The nominal sensitivity of the piezoelectric strain sensor with impedance converter and range capacitor is 35.430 mV/με. The use and layout of these items will be further discussed in the section 3-3-2.

3-1-3-Piezoelectric Accelerometers

Figure 7: Piezoelectric accelerometer sensors

Eight integrated circuit piezoelectric accelerometers are installed on the test bridge. Traditionally, accelerometers are used mainly in bridge health monitoring. This dual-purpose system was designed to include accelerometers both for the traditional bridge health monitoring measurements and for exploratory application and further

comparison to the bridge weigh-in-motion results from the strain gages.

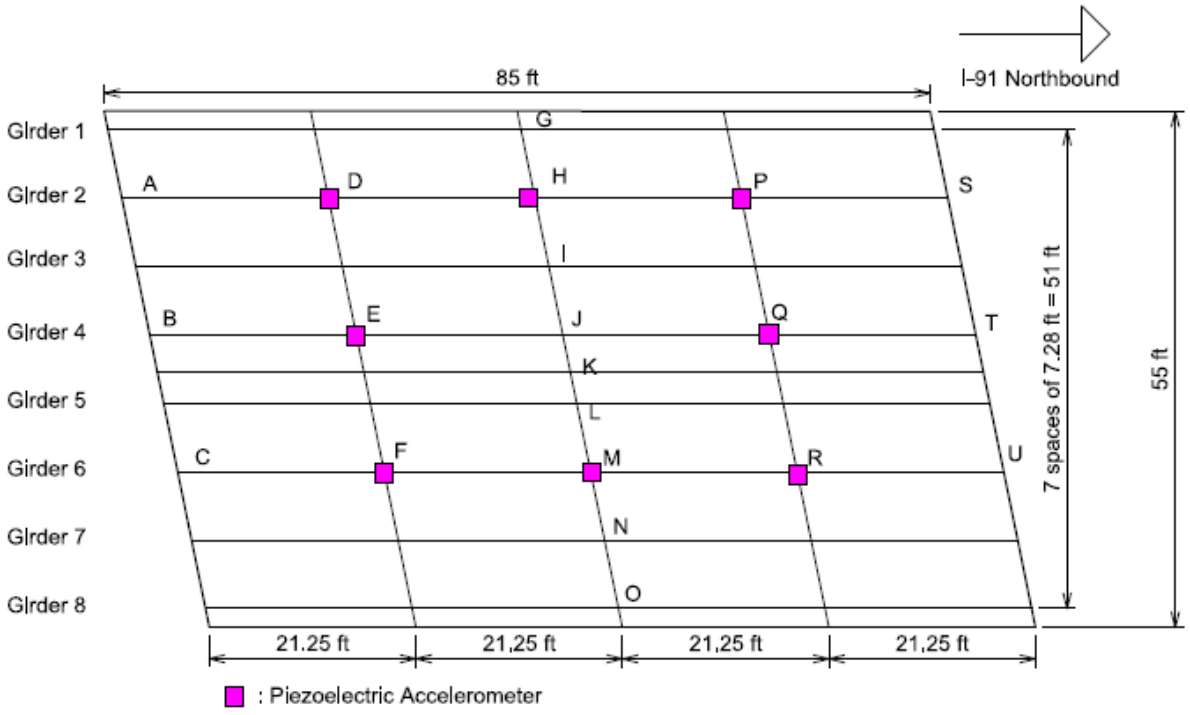

Figure 8: Plan view of piezoelectric accelerometer sensors layout

Figure 7 shows an image of the piezoelectric accelerometer, manufactured by PCB Piezotronics, Inc. The piezoelectric accelerometers have a ±0.25 g peak acceleration level and a frequency range from 0.1 to 200 Hz. According to specifications, the sensitivity is nominally 10.0 V/g and the resonant frequency is a minimum of 700Hz. Sensors are located at each of the quarter-spans, for girders 2, 4, and 6 and also at the midspan of girders 2 and 6. The layout for the piezoelectric accelerometer sensors is shown in Figure 8. Accelerometers are installed at quarter and mid-span over the bridge, primarily for BHM purposes.

After an initial data collection test period, it was determined that an accelerometer with a larger frequency range may provide results that could better capture when trucks entered onto and left the bridge. New piezoelectric accelerometers with frequency range

of 0.15 to 1000 Hz were installed increasing the upper frequency range from 200 Hz to 1000 Hz. These new accelerometers, are Model 393B12 manufactured by PCB Piezotronics (Fig. 9).

Figure 9: Piezoelectric accelerometer sensors with frequency range of 0.15 to 1000 Hz (picture from vendor)

3-1-4-Capacitance Accelerometers

Figure 10: K-Beam Variable capacitance accelerometer

Four capacitance accelerometers are installed on the Meriden Bridge (Fig. 10), at the mid-span of girders 2 and 6 and quarter-span of girder 4, as shown in Figure 11. They are collocated at four of the eight locations with the piezoelectric accelerometers. These sensors measure the temperature of the sensor as well as the vertical acceleration.

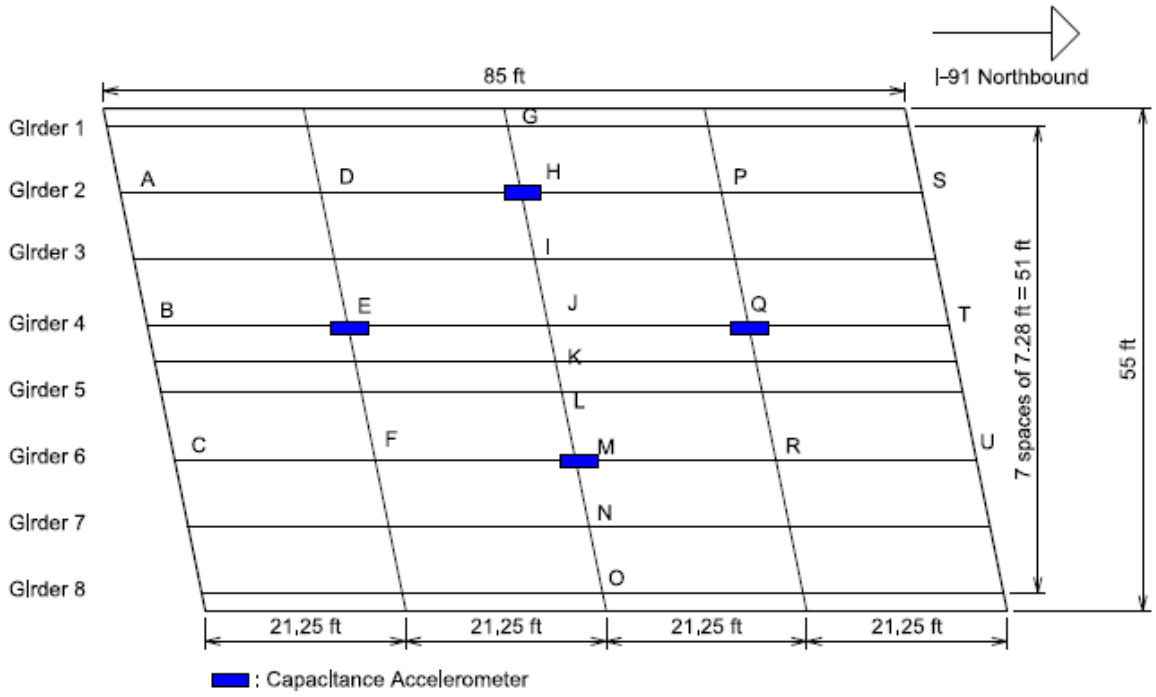

Figure 11: Plan view of capacitance accelerometer sensor layout

The capacitive accelerometers have a measurement range of ±2 g and a frequency range of 0 to 250 Hz. The sensitivity is nominally 1000mV/g (q1 V/g) and the resonant frequency is 1400Hz. The K-Beam variable capacitance accelerometers are manufactured by Kistler Instruments, Inc.

3-1-5-Resistance Temperature Detectors

Four temperature sensors are installed at two quarter-spans of girder 4 and mid-spans of girders 2 and 6 (Fig. 12). This diamond configuration will show if there are significant temperature changes between the east and west direction across the bridge or in the north to south direction along the bridge. The climate in Connecticut includes a very wide range of temperatures throughout the year. The system was designed to collect temperature measurements to assess and account for the variability and impact of the field conditions to both health monitoring and weigh-in-motion.

The temperature sensor is a general purpose Resistance Temperature Detector (RTD) that is surface-mounted underneath the bridge.

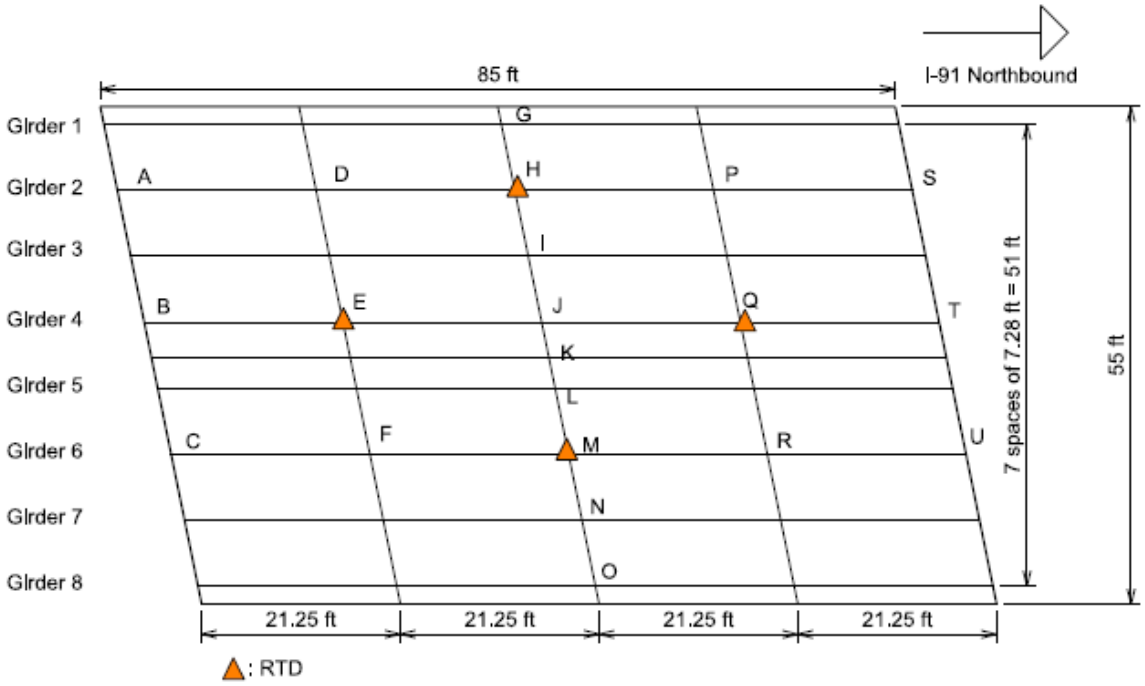

Figure 12: Plan view of resistance temperature detectors layout

The RTD sensor, shown in Figure 13, is manufactured by Pyromation, Inc.

Figure 13: Resistance temperature detector sensor

3-1-6-Microphone

A pre-polarized random-incidence condenser microphone with frequency range of 15 Hz - 12.5 kHz is installed at the Meriden Bridge. It is mounted on the traffic cabinet

located at the abutment on the bridge approach (South end). This microphone was selected to measure global bridge vibrations and to evaluate high frequency capabilities. The potential to use sound characteristics for calculating the speed of the trucks and other bridge output will be explored. The microphone is shown in Figure 14.

Figure 14: Microphone to measure global vibration of bridge

3-1-7-Video Camera

A video camera is mounted on a utility pole next to the Meriden Bridge to capture images of vehicles crossing the bridge. Image capture can be triggered based on bridge response criteria. The image collection is synchronized with the bridge data collection. The system was instrumented with a camera for the primary purpose of validating vehicle type and traffic configuration for the purposes of the test.

The camera is an "acA2000-50gc" Model, manufactured by Basler Inc. (shown in Fig. 15). The frame rate per second (fps) is 50 with pixel size of 5.5µm×5.5µm. The camera is mounted in a field housing for weather protection.

Figure 15: Video Camera to capture image of vehicles (picture from vendor)

3-2-System Components

3-2-1-Computer

The computer used for data collection is a Dell™ Ultra Small Form Factor-Optiplex™780 (Fig. 16) with a Windows® 7 Professional 64-bit operating system. Specifications for the computer include 3.33GHz Intel® Core™ 2 Duo E8600 processor, a 320GB 7,200 RPM SATA hard drive and 4GB of memory. The computer is located in a traffic cabinet, as shown in Figure 16. Also in the cabinet is a Dell Professional P170S 17 inch monitor, 9.4 by 9.3 inches and 2.6 inches deep.

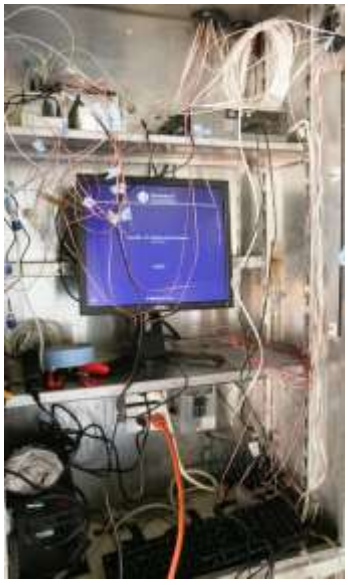

Figure 16: Computer for data acquisition at Meriden Bridge

3-2-2-Data Acquisition Unit

Figure 17: Cabinet housing system components under Meriden Bridge

The data acquisition system components are housed in a converted traffic signal cabinet as shown in Figure 17. The cabinet is located on the southern abutment underneath the bridge. There is an air filter installed in the cabinet.

A data acquisition unit will provide signal conditioning and high sampling rates for a wide range of sensors. The BHM and BWIM methods are implemented automatically on a PC at the bridge site. The PC, located in a cabinet mounted on the bridge abutment, will be remotely accessible using a cellular modem.

3-2-3-Data Acquisition Hardware

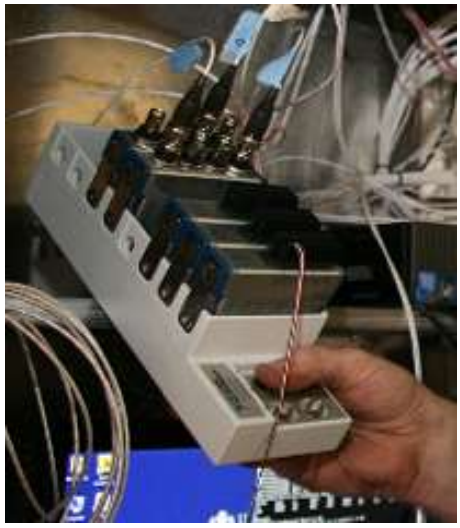

Figure 18: NI cDAQ-9178 CompactDAQ Chassis

The data acquisition hardware is a National Instruments (NI) NI cDAQ™-9178 CompactDAQ chassis with associated modules (Fig. 18). The chassis has 8 slots for modules and is connected to the computer using a USB 2.0 Hi-Speed cable. Resolution of the chassis is 32-bits. Dimensions of the chassis are 10 inches by 3.47 inches by 2.32 inches.

MATLAB® software that includes an add-on Data Acquisition Toolbox is installed on the computer. This enables collection and data analysis using MATLAB.

3-2-4-Data Acquisition Modules

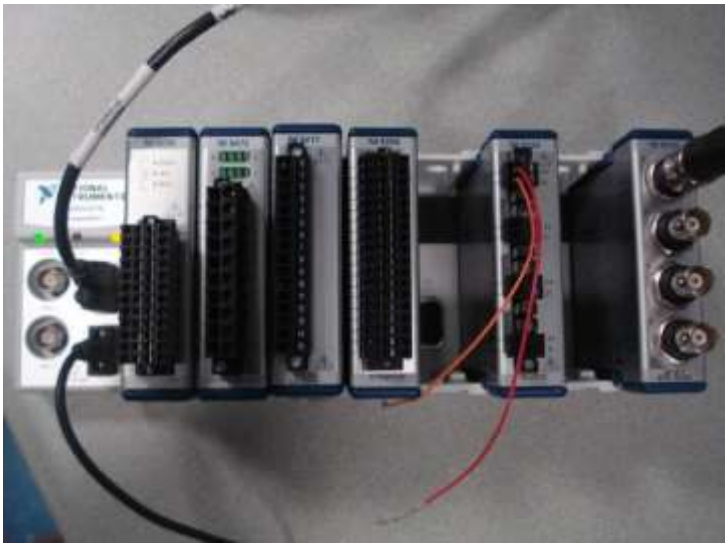

Figure 19: Data acquisition modules

There are five different types of data acquisition modules in use at the Meriden Bridge. All modules are made by National Instruments and can be inserted into the slots of the DAQ chassis discussed in Section 3.2. Figure 19 provides an example of how modules are installed in a DAQ chassis. (Note: Figure 19 is not the actual module arrangement used at the Meriden Bridge chassis.) Resolution for the data acquisition modules is 24-bits, except for the NI 9206 module that has 16-bit resolution.

Figure 20: NI 9236 module for collection of foil Strain gages data

The quarter bridge foil strain gages data are collected by the NI 9236 module. Each module can collect from eight simultaneous channels, or sensors. For the eighteen strain gages there are three of these modules. They are installed in slots 1-3. The maximum sample rate is 10 kS/s per channel with 1000Vrms transient isolation. The NI 9236 is shown in Fig. 20.

Figure 21: NI 9234 module for collection of piezoelectric accelerometers/strain gages data

The piezoelectric accelerometers and piezoelectric strain sensors data are collected using the NI 9234 IEPE accelerometer module. For this module the IEPE is software selectable at 0 or 2 mA and the coupling is software selectable AC/DC coupling. For operation of both the piezoelectric accelerometers and piezoelectric strain sensors the settings are 2 mA and AC coupling. The NI 9234 has the capability to sample at a maximum rate of 51.2 kS/s per channel. The eight accelerometers require two of these 4 channel modules. The four strain sensors require one additional 4 channel module. Two views of the NI 9234 are shown in Fig. 21.

Figure 22: NI 9206 module for collection of capacitance accelerometer data

The NI 9206 can have up to 16 differential channels or 32 single ended channels. For the four capacitive accelerometers eight single ended channels are used for the 4 accelerations and 4 temperature measurements. The maximum sampling rate is 250 kS/s aggregate sampling rate. Figure 22 shows the NI 9206 on the left, as well as an NI 9472 on the right

Figure 23: NI 9217 for collection of temperature sensors data

The NI 9217 4-Ch PT100 RTD collects the four temperature sensor signals. Each module can collect from four differential sensors. The module can either be used at 100 S/s per channel for fast sampling rates, or at 1.25 S/s per channel with a built-in 50/60 Hz noise rejection. Two views of the NI 9217 are shown in Figure 23.

Figure 24: NI 9232 for collection of piezoelectric strain gages data (picture from vendor)

The NI 9232 collects piezoelectric strain sensors data (Fig. 24). This module has a lower cutoff frequency (-3dB at 0.1 Hz; -1dB at 0.87Hz) when in AC coupling mode compare to NI 9234. The NI 9232 is a 3-channel C Series dynamic signal acquisition module for making industrial measurements from integrated electronic piezoelectric (IEPE) and non-IEPE sensors. This module delivers 99 dB of dynamic range and incorporates software-selectable AC/DC coupling and IEPE signal conditioning for accelerometers, tachometers, and proximity probes. The three input channels simultaneously digitize signals at rates up to 102.4 kHz per channel with built-in antialiasing filters that automatically adjust to a desired sampling rate.

3-2-5-USB Mobile Broadband

Figure 25: USB mobile modem (picture from vendor)

An internet connection is provided using a Sprint® 3G/4G USB Modem 250U by Sierra Wireless. It can rotate for optimum connectivity with 3G average download speeds between 400 and 700 Kbps. When 4G coverage is available to download speeds are ten times faster than when using 3G coverage. Dimensions are 0.6 inch depth by 1.9 inch diameter. The modem plugs into the back of the computer in an available USB port. Figure 25 shows the USB mobile modem device.

3-2-6-Digi Connect WAN 3G modem

The Digi Connect® WAN family of commercial-grade Wireless WAN cellular routers is being replaced with the USB modem to provide a steadier internet connection to the monitoring system. Figure 26 shows the Digi modem which is supported by Sprint network provider. This modem provides secure high-speed wireless connectivity to remote sites and devices.

Figure 26: Digi Connect WAN 3G modem (picture from vendor)

3-3-Sensor Connections to System Components

Further information provided in this section on the connections includes sensor mounting methods, sensor connections to the cable, and cable attachments to the data acquisition modules. The wiring for the sensors is all contained within fiberglass conduit attached directly to the bridge abutment and underside of the bridge deck.

3-3-1-Foil Strain Gage Connection to System

Foil strain sensors are mounted by welding to the girder. The location to be welded must be pretreated using a grinder and degreaser to ensure a smooth surface connection. Next, the sensor is spot welded in place. Full installation instructions from Vishay can be found in Appendix A.1. An installed foil strain gage is shown in Fig. 27.

Figure 27: An installed foil strain gage on the Meriden Bridge

The sensor has five feet of the three wire cable already attached to it. To get to a desired length, additional cable is soldered wire by wire and then wrapped with a shrink tube for protection from the elements.

The three wires of the quarter bridge foil strain sensor attach to NI 9236 module. The black wire connects to the excitation (EXC), the white wire connects to the analog input (AI), and the red wire connects to the (RC) designated spots in the module.

3-3-2-Piezoelectric Strain Gage

Figure 28: Magnetic mount to install piezoelectric strain sensors

A mount is developed specifically for the piezoelectric strain gages. Traditionally they are mounted by drill and tap with a countersunk screw. To avoid making a hole in the girder of a bridge to be monitored, a magnetic mount is used (Fig. 28). The magnetic mount consists of 4-6 magnets (depending on available space) with 80 lbs pulling force for each magnet for a total of 320 lbs – 480 lbs. Kistler specifies the torque required for the M6 bolt used to secure the strain sensor at 7.4 lb-ft (10 Nm). The required normal force can be determined by dividing the required torque by the product of 0.1 and the diameter of the M6 bolt (approximately 0.2 in, 5 mm). The resulting normal force is estimated in this manner as 4,500 lbs (20 kN). The specified torque assumes a 600μs strain range. The anticipated strain range is less than 40μs which would allow the normal

force to be scaled accordingly to 300 lbs. This is achieved by only four magnets. A 1 inch by 12 inch by 0.25 inch steel bar is bridged over the magnets. A screw threaded through the steel bar is used to apply the normal force onto the sensor.

There is a one foot length green cable attached to the sensor, and attached on the other end to the model 571A5 range capacitor and model 558 impedance converter. A general purpose cable with BNC connector is then connected between the impedance converter and the NI 9234 module.

3-3-3-Piezoelectric Accelerometer

Junction boxes in the conduit are mounted to the bottom of the concrete bridge deck using a hammer drill and screws ensuring that the junction box is firmly fixed to the underside of the deck. The accelerometers are mounted inside the junction boxes with threaded studs screwed into holes drilled and tapped into the junction box itself.

From the sensor, there is a 2-pin top connection that connects to a one foot length 2-socket boot connector to BNC jack cable. This one foot cable then connects to a BNC to BNC cable ordered to desired length. The BNC end simply screws into the AI terminal of the NI 9234 module.

3-3-4-Capacitance Accelerometer

The capacitance accelerometers are also located in the junction boxes under the bridge deck. These sensors are attached to a plastic piece that is drilled and taped to accept the capacitance accelerometer. The plastic piece is glued to the inside of the junction box.

Figure 29: A power supply to power the capacitance accelerometers (picture from vendor)

The output cables are attached to the sensor by twist connection. A power supply type B24G30 produced by Acopian Company was used to provide the required power for capacitance accelerometers (Fig. 29). The power supply B24G30 contains five external screw/ports including +out, -out, LAC, NAC, and ground. Three ports including LAC, NAC, and ground are used to connect the power supply to the power cord. The capacitance accelerometer cable has four wires including power (red wire), acceleration signal (white wire), temperature signal (yellow wire), and ground (black wire).The power wire of capacitance accelerometer is connected to the +out of power supply via the red lead wire. The signal wires of capacitance accelerometer are connected to the channels of NI 9206 via the white and yellow wires. White and yellow wires are collecting acceleration and temperature signals, respectively, in the capacitance accelerometer. The common ground of NI 9206 module (COM) and ground wire of capacitance accelerometer (black wire) both are connected to the –out of power supply.

3-3-5-Resistance Temperature Detector

Figure 30: An installed resistance temperature detector on the Meriden Bridge

Locations on the girder for temperature sensors must be prepped and cleaned similarly to the locations of strain sensors. Then the temperature sensors are mounted to the girder using the epoxy. Figure 30 shows one of the installed temperature sensors on the Meriden Bridge.

The RTD sensors have integrated cables. The cable length can be specified and ordered to desired length. The output end of the cable has four wires, two are red and two are white wires. These connect to the NI 9217 module. The red wires are attached to the terminals for excitation (EX) and RTD+. The white wires are attached to the spots for RTD- and common (COM).

4-BWIM

4-1-BWIM methodology

The BWIM methodology uses strain measurements from the steel girder of the slab-on-girder highway bridge to determine gross vehicle weight, speed, axle spacing and axle weights. The method does not require development of a bridge model or influence line. The unique aspect of the proposed BWIM method in this study is the non-intrusive

(i.e. no sensors in the pavement) calculation of truck characteristics for a single-span highway bridge, using only strain measurements of the steel girders beneath the bridge. The proposed method builds on the theory for determining gross-vehicle weight from the work of Ojio and Yamada *(*Ojio and Yamada, 2002*)* and the findings of Cardini and DeWolf (2009). It is further documented in Wall et al. (2009).

The BWIM method employed here assumes that the single-span bridge behaves as a simply supported beam neglecting the spatial behavior of the multi-lane bridge; assumes the truck loads are applied to the bridge by the truck axles and can be modeled as a group of point loads moving across the simply supported beam at fixed spacing and constant speed; and neglects both bridge and truck dynamics.

The unique aspect of this method is the use of the second time derivative of the measured strain to identify, with large negative spikes or peaks, when the truck axles pass over the center of bridge. Truck speed is determined from the time, t_1, it takes the first-axle of the truck to travel from the start of the bridge to the mid-span of the bridge such that

$$v = \frac{L}{2(t_1)} \tag{1}$$

Where v is the speed of the truck (ft/sec), L is the length of the bridge (ft) and t_1 is the time it takes for the first axle of the truck to travel from the start of the bridge to the mid-span (sec). The sensors can be located at any location along the length of the bridge and, as observed from the theory of influence lines, will read peak strain values when the point load crosses the center of the bridge. It is optimal to place the strain sensors at the center of the bridge as this provides the largest amplitude of strain response.

The second derivative of the strain also provides the times when each of the remaining axles pass over the mid-span of the bridge; t_2, t_3, t_4 and t_5 for a 5-axle truck. The product of time difference between these times and the calculated speed provides the truck's axle spacing, x_n, as given by

$$x_n = v(t_{n+1} - t_n), \qquad n= 1,2,\ldots,N\text{-}1 \tag{2}$$

where x_n is the distance between the *n-1* and n^{th} axles, and t_n is the time it takes for the n^{th} axle to reach the mid-span of the bridge after the truck first enters the bridge, and N is the total number of axles of the truck.

Gross vehicle weight is then determined from the method of Ojio and Yamada, (2002) as described subsequently. The *response wave* is the strain response of the bridge to a truck traveling over the bridge. The response wave can be defined mathematically as the strain at a specific location of the bridge due to multiple point loads traveling over the bridge. The response wave is written as

$$\varepsilon(x) = \sum_{n=1}^{N} P_n f(x - x_n) \tag{3}$$

Where P_n is the weight, or magnitude, of the n^{th} axle, assumed to be a point load, x_n is the distance between axles, and $f(x - x_n)$ is the influence line of the simply supported beam. The influence area, A, of a single truck passing over the bridge is defined as

$$A(x) = \int_{-\infty}^{\infty} \varepsilon(x) dx \tag{4}$$

Substituting Eq. 3 into Eq. 4 and rearranging slightly gives

$$A = \sum_{n=1}^{N} P_n \int_{-\infty}^{\infty} f(x - x_n) dx \tag{5}$$

Recognizing that the Gross Vehicle Weight (GVW) can be written as

$$GVW = \sum_{n=1}^{N} P_n \tag{6}$$

allows Eq. (5) to be simplified as

$$A = GVW \sum_{n=1}^{N} \int_{-\infty}^{\infty} f(x - x_n) dx \tag{7}$$

For trucks with the same axle configuration the term in the summation is a constant, such that

$$\alpha = \sum_{n=1}^{N} \int_{-\infty}^{\infty} f(x - x_n) dx \tag{8}$$

This constant α can be substituted into Eq. (7) and written as

$$\frac{A}{GVW} = \alpha \tag{9}$$

This method requires the GVW of a test truck to be known and then the GVW of any *unknown* weight truck can be determined knowing that

$$\frac{A_k}{GVW_k} = \frac{A_u}{GVW_u} \tag{10}$$

where A_k and GVW_k are the calculated area and reference gross vehicle weight for a test truck of *known* weight, and A_u and GVW_u are the calculated area and gross vehicle weight for a truck with *unknown* weight. Equation (10) can be arranged so that

$$GVW_u = \frac{A_u}{A_k} GVW_k \tag{11}$$

The ratio of GVW_k to A_k is defined as the calibration constant β where

$$\beta = \frac{GVW_k}{A_k} \tag{12}$$

Thus, the GVW of the unknown truck is then determined as

$$GVW_u = A_u \beta \tag{13}$$

Where *A* can be written in terms of ε(t), again where $x = vt$, and written in discrete form such that

$$A(t) = v \int_{-\infty}^{\infty} \varepsilon(t) dt = \frac{v \Delta t}{M} \sum_{i=1}^{M} \varepsilon(i \Delta t) \tag{14}$$

where Δt is the discrete sample time of the strain measurement, and *M* is the total number of measurements needed for the truck to cross the bridge. The axle weights are relative to the magnitudes of the peaks of the second time derivative of the strain as each axle passes over the center of the bridge span. In practice BWIM is often conducted over a short period of time where temperature variation can be neglected. For a system that will be in-place through seasonal variations the effect of the temperature should be examined. In this study, temperature measurements at multiple locations will be used to assess the effect of temperature variations and thermal gradient on the accuracy of the BWIM data.

4-2-Field study

A pilot study, conducted on December 13, 2011, included an initial field test using a loaded 5-axle truck of known weight making multiple passes over the prototype bridge system. The purpose of this initial field test was for initial calibration of the BWIM method. A secondary purpose of the pilot study was to gather information on the various sensor responses, assess the ability to calculate speed data and evaluate the variability in the results from applying the calibration to the initial test vehicle calculations.

4-2-1-Truck of known weight

The test vehicle was a five-axle semi-trailer with air-ride suspension (Fig. 31). The vehicle was loaded, and then was measured to weigh 68,600-lbs (31116-kg). The static weight was obtained at the weigh station on I-91 northbound in Middletown prior to testing, operated by the State Police. A total of twelve passes were made by the truck during the field test: five passes in the middle lane and seven passes in the slow lane. The truck driver attempted to vary the speed at 50-mph (80-kph), 55-mph (88-kph), and 60-mph (96-kph) according to instructions and based on traffic.

Figure 31: Truck of known weight

4-3-Test results and evaluation

The speed of the truck was recorded both from reading a commercial navigation system installed in the truck and derived from a portable GPS unit incorporating radar, receiver and aerial map installed in the truck for the purpose of this study. The speeds collected from both GPS based devices were well correlated with a maximum difference of 1 mph. Therefore the speed recorded from the commercial navigation system was used as the "ground-truth" or "actual" truck speed for comparison with the speed calculated from the bridge response. The speed of the truck was calculated based on bridge strain data and using Equation (1). A comparison between the measured (GPS)

and calculated (bridge) speeds is presented in Table 1. The average difference between measured and calculated speed was 4.5% and indicates that the calculated speed was in reasonable agreement with that recorded by the "actual" speed data.

Table 1- Comparison of Measured and Calculated Truck Speed

Run	Lane	Attempted Speed* (mph)	Measured Speed (mph)	Calculated Speed (mph)	Difference%
1	Middle	60	58	62	6.5
2	Middle	60	62	66	6.6
3	Middle	60	62	65	4.8
4	Middle	60	63	65	3.1
5	Middle	60	63	66	4.2
6	Slow	60	62	65	5.3
7	Slow	60	61	62	2.3
8	Slow	60	62	64	2.9
9	Slow	60	62	57	7.5
10	Slow	60	63	65	3.5
11	Slow	55	55	57	4.1
12	Slow	50	49	51	3.9

* the attempted speed is the speed the driver was instructed to drive.

The performance of the two accelerometer technologies, piezoelectric and capacitive, is examined in the time domain and frequency domain as shown in Figs. 32(a) and (b). The data shown are from accelerometers placed on girder 6 at mid-span with the truck traveling in the slow lane at a speed of 62-mph (100-kph). An eight-pole low-pass filter with a 100 Hz cutoff frequency was used to reduce the effect of noise on the acceleration data. The piezoelectric and capacitive accelerometers have a frequency range of 0.1 to 200 Hz and 0 to 250 Hz, respectively. From the time domain plots the two accelerometers are observed to have similar noise levels and provide comparable measurements. A time lag of 0.019 seconds was observed in the capacitive accelerometers relative to the piezoelectric accelerometers (inset in Figure 32(a)). In the

frequency domain the two sensor technologies provide similar performance above 3 Hz, while the piezoelectric accelerometer rolls off at lower frequencies. Neither accelerometer can capture the crossing of truck axles over the midspan. It is expected that accelerometers with larger bandwidth will be able to measure this large negative acceleration when the axles pass over the center of the bridge and can be used as redundant or replacement measurements for the truck speed. Piezoelectric accelerometers with higher frequency range were installed to examine the benefit of larger bandwidth for the acceleration measurements.

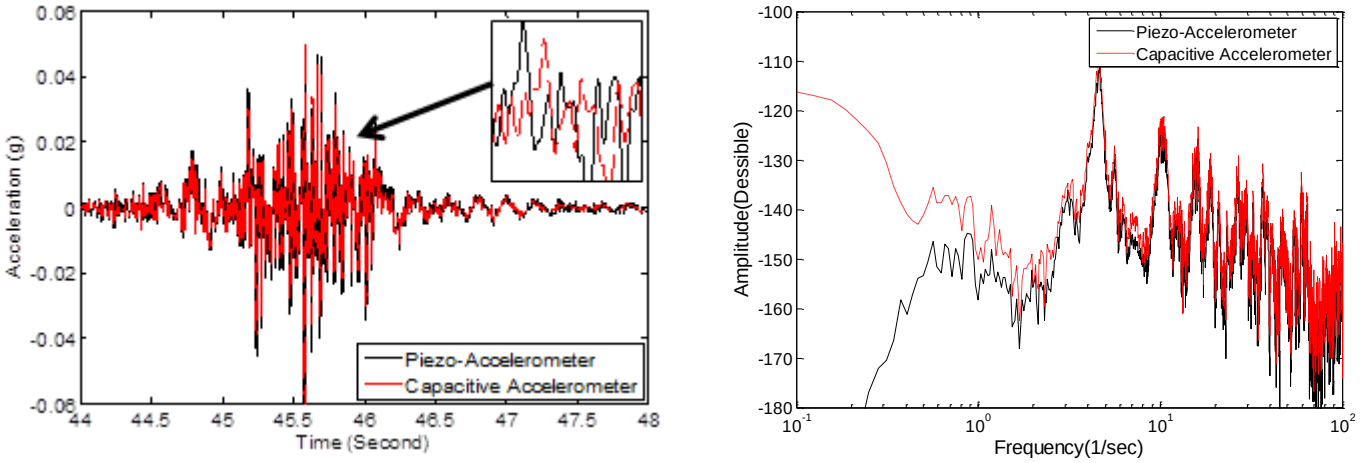

(a) (b)

Figure 32: Piezoelectric accelerometer vs. capacitive accelerometer data: (a) time history for truck crossing; (b) auto power spectral density of acceleration.

The performance of the two types of strain gage technologies, foil strain gage and piezoelectric strain gage, are compared in Figs. 33(a) and (b) in the time domain and frequency domain, respectively. These data are measured from the gages on girder 6 at the North bearing. A comparison in time domain shows the time decay observed in the piezoelectric strain gauge signals resulting from the signal conditioner used for this sensor. The attenuation at low frequencies was observed in the frequency domain as

well. The data from both sensor technologies are in good agreement from 0.5-10 Hz. A large peak in the autopower spectral density functions of both strain sensors was observed at 60 Hz corresponding to ground loop noise. An eight-pole low-pass filter with a 30 Hz cutoff frequency was applied to reduce the effect of the ground loop noise at 60 Hz. The strain measurements from the foil-type strain sensors are used for the BWIM measurements in this report.

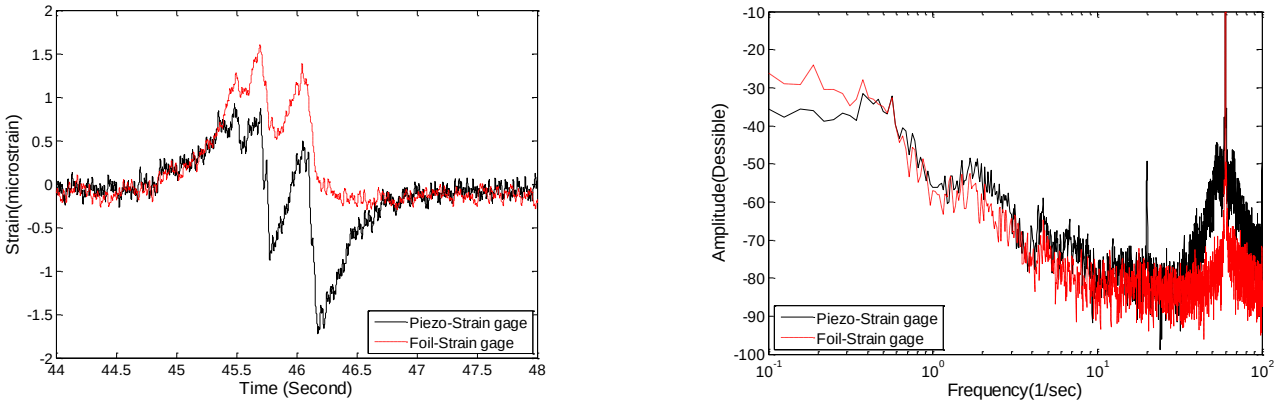

(a) (b)

Figure 33: Piezoelectric strain sensors vs. foil Strain gages data: (a) time history for truck crossing; (b) autopower spectral density of acceleration.

The axle spacing of the test truck is calculated using the calculated speed and Equation (2) with time intervals based on the large negative spikes in the second derivative of the strain history, as shown in Fig. 34. Table 2 presents the measured and calculated axle spacing for the middle lane and slow lane. The prediction of axle spacing for Run 6 is incomplete for the last three axles due to the presence of multiple vehicles on the bridge. The axle spacing is slightly overestimated in comparison to actual measurements, due to an overestimation bias in the speed calculation, as observed in Table 1. This overestimation demonstrates both the sensitivity and importance of the speed calculation.

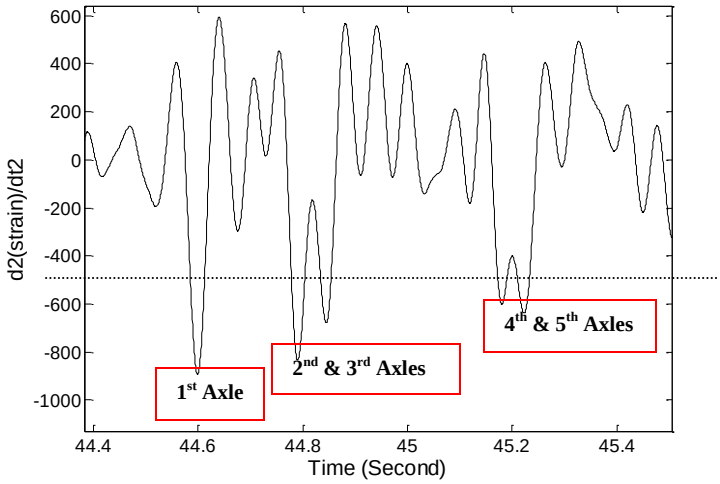

Figure 34: Negative spikes in second derivative of strain measurement when the truck axles pass over the mid-span of the bridge

For calibration, the ratio of GVW_k to A_k, called β, is calculated from Equation (12) for each pass in the middle lane and each pass in the slow lane, based on the static weight of the truck (68,600-lb) and the measured strain at the midspan of girders 6 and 4, respectively. The calibration constant β calculated (as the average of these values), is 0.032-lb/ft for the middle lane, and 0.034-lb/ft for the slow lane. The standard deviation of β is 0.0036-lb/ft, which demonstrates the repeatability of the method.

Table 2- Comparison of measured and calculated truck axle spacing

Axles	Meas. Ft (meter)	Calculated (Middle Lanes) ft (meter)					Calculated (Slow Lanes) Ft (meter)						
		1	2	3	4	5	6	7	8	9	10	11	12
1 to 2	**17 (5.1)**	17.6 (5.4)	17.9 (5.4)	17.7 (5.4)	17.6 (5.4)	17.7 (5.4)	17.1 (5.2)	17.4 (5.3)	17.3 (5.3)	17.3 (5.3)	17.4 (5.3)	17.4 (5.3)	17.5 (5.3)
2 to 3	**4.2 (1.3)**	5.3 (1.6)	5.4 (1.6)	5.3 (1.6)	5.7 (1.7)	6 (1.8)	*	5.5 (1.7)	5.7 (1.7)	5.6 (1.7)	5.4 (1.6)	5.5 (1.7)	5.4 (1.6)
3 to 4	**30.6 (9.3)**	31.7 (9.6)	31 (9.4)	31 (9.4)	30.6 (9.3)	31.7 (9.6)	*	31 (9.4)	30.5 (9.3)	34.4 (10.5)	31.1 (9.5)	31.1 (9.5)	30.6 (9.3)
4 to 5	**4.1 (1.2)**	5.5 (1.7)	5.5 (1.7)	5.3 (1.6)	5.4 (1.6)	5.4 (1.6)	*	5.3 (1.6)	5.5 (1.7)	5.4 (1.6)	12.4 (3.7)	5.5 (1.7)	5.2 (1.6)

"*" issues due to presence of multiple trucks on the bridge

Based on the selection of β, the weight of the truck of known-weight for different runs is calculated using Equation (13). These results are presented in Table 3. The measured and calculated weight of the truck are in a well agreement in most of the cases and the average difference between the calculated and measured weight was respectively, 8.0% and 7.8 % for the middle and slow lanes. While these weights were calculated using the constant β, calculated from the same data set, the weight data are useful to ascertain the variation when applied to the variation from the test truck. Applying this technique, the outcome was a comparable β. Additional test runs are planned to apply the calibration factor, β, to different vehicles and a larger number of vehicles.

Table 3- Comparison of measured (68,600-lb (3116-kg)) to calculated truck weight

	Middle Lane					Slow Lane						
Runs	1	2	3	4	5	6	7	8	9	10	11	12
Weight lb (kg)	66551 (30187)	68780 (31198)	62120 (28177)	65157 (29554)	84206 (38195)	70008 (31755)	59488 (26983)	70538 (31995)	64001 (29030)	66805 (30302)	85386 (38730)	70488 (31972)
Difference%	2.99	0.26	9.45	5.02	22.75	2.05	13.28	2.83	6.7	2.62	24.47	2.75

5-BHM

5-1-BHM methodology

To account for the variability associated in calculating the desired damage measure, a probabilistic BHM approach can be adopted to detect global damage in the highway bridge. This section defines damage measures used to identify structural changes in the bridge structure, describes the probabilistic framework used to assess any changes in the bridge condition, and presents a means to incorporate temperature and truck weight data in the probabilistic framework to enhance the accuracy of the BHM.

In order to assess the structural integrity of the bridge, damage measures (DMs) corresponding to the structural health of the bridge are determined from the structure's dynamic response to truck traffic. The basis for this method is that a healthy DM (DM_H) can first be determined as a baseline. At subsequent times, the current DM (DM_C) can be determined and compared to the healthy case. For this bridge the DMs, similar to those used in Cardini and DeWolf (2009), are the peak strain, strain distribution over the eight steel girders, calculated location of neutral axis, and estimated fundamental natural frequency of the bridge which is calculated as the first peak of the power spectral density function (PSD).

The first damage measure is the peak strain measured at the bottom of the eight steel girders each time a truck crosses. The peak strain damage measure is determined as the strain in each of the eight girders at the time, t_{pk}, of the maximum peak strain over all of the girders. The first damage measure can be determined as

$$DM_i^1 = \varepsilon_i\left(t_{pk}\right) \tag{15}$$

where DM_i^1 is the peak strain on all eight girders $i=1,2,...,8$ at the time t_{pk}, ε_i is the strain reading of the bottom strain sensor at the midspan of each girder. If the peak strain increases, this can be an indication of local damage (e.g. fatigue cracking) or damage in an adjacent girder; whereas, if the peak strain decreases, this can indicate damage somewhere on the length of that girder.

The second damage measure is the distribution of the strain in the eight girders as a truck passes over the bridge. This DM is an indicator of how the load is distributed to each of the girders of the indeterminate structural system. The strain distribution is determined as

$$DM_i^2 = \frac{\varepsilon_i\left(t_{pk}\right)}{\sum_{i=1}^{8}\varepsilon_i\left(t_{pk}\right)} \tag{16}$$

Where DM_i^2 is the distribution factor for the i^{th} girder. If the strain distribution changes, this is an indication that the load path of the indeterminate structural system of the bridge has changed and members under less strain may be damaged, while members under larger strain are likely undamaged (or less damaged).

The third damage measure is the location of the neutral axis at each girder. If the neutral axis rises into the slab there can be tension and cracking of the concrete bridge deck. If the neutral axis lowers there could have already been failure of the deck.

$$DM_i^3 = d_i - \frac{\varepsilon_i\left(\hat{d}_i - d_i\right)}{\left(\hat{\varepsilon}_i - \varepsilon_i\right)} \tag{17}$$

where DM_i^3 is the distance from the bottom of the girder to the neutral axis, d_i is the distance from the bottom of the girder to the bottom sensor, $\hat{d}_i$ is the distance from the bottom of the girder to the top sensor, and $\hat{\varepsilon}_i$ is the strain reading at top sensor of each girder.

The final damage measure considered in this study will be the measured bridge natural frequencies.

$$DM_j^4 = f_j \tag{18}$$

where the natural frequencies f_j are determined from the peaks of the auto-power spectral density functions of the measured acceleration responses as given by (Bendat and Piersol, 2000)

$$G_{xx}(f) = 2\lim_{T\to\infty}\frac{1}{T}E\left[\left|\ddot{X}_k(f,T)\right|^2\right] \tag{19}$$

where G_{xx} is the auto-power spectral density function of *x(t)*, *T* is the record length taken to be a sufficiently long record, *E* is the expected value operator, and $\ddot{X}_{(k)}$ is the finite Fourier transform of the measured acceleration $\ddot{x}(t)$ for the k^{th} ensemble. The bridge natural frequencies are directly related to the mass and stiffness of the bridge structure. Therefore, a change in the natural frequency is an indicator that the stiffness (or mass) of the structural system has changed.

5-2- Probabilistic approach

The DMs, calculated from measured bridge responses from traffic loading, are neither deterministic nor constant and can be considered to be random variables with a Gaussian distribution. As such, not just one realization of each DM is calculated, but a set of *n* DMs are determined. The mean and variance of the original set of data for the *healthy* structure is determined so that the probability density function of DM_H is known. At each *current* period of time, *n* new DMs are calculated and the mean and variance are determined as before so that the probability density function of DM_C is now known. The basis for this probabilistic method is then to compare the distribution of a current DM to the baseline DM to determine if there is a change in the underlying distribution, thus indicating a potential change in the structure and possible damage *(23)*.

The Student's t-test is used to compare the two distributions of each of the DMs. It is assumed that the variance of the two samples is unequal and an adaptation of the Student's t-test called Welch's t-test is used. Welch's t-test defines the statistic *t* as

$$t = \frac{\overline{X}_H - \overline{X}_C}{s_{\overline{X}_H - \overline{X}_C}} \tag{20}$$

where

$$s_{\bar{X}_H - \bar{X}_C} = \sqrt{\frac{s_H^2}{n_H} + \frac{s_C^2}{n_C}} \tag{21}$$

$\bar{X}_H$ and $\bar{X}_C$, s_H^2 and s_C^2, and n_H and n_C are the mean, variance, and sample size, respectively, of the healthy and current distributions.

The t-distribution can be used to test the null hypothesis that the two DM means are equal at a certain significance level. If the current t-statistic is less than the critical *t* value for a particular level of significance, the null hypothesis is rejected; this indicates a statistically significant change in the mean and potential for damage in the structure. If the current t-statistic is greater than the critical t value for a particular level of significance, the null hypothesis cannot be rejected; this indicates no statistically significant change in the mean and that the structural integrity of the current scenario should be assumed the same as the structural integrity of the baseline scenario.

To provide further insight into the statistical test, the p-values instead of a general 'pass' or 'fail' result are observed. The p-value is the probability of observing an event at least as extreme as the one actually observed, given that the null hypothesis is true. The p-value for a two-tailed Welch's t-test can be calculated as:

$$p = 2[1 - \Phi(t)] \tag{22}$$

where Φ is the standard normal operator. Generally one rejects the null hypothesis when the p-value is smaller than or equal to the significance level.

5-3-Accounting for thermal and truck weight effects in BHM

While the probabilistic approach can accommodate inherent variability in the system, the ability to identify structural damage can be enhanced by accounting for the variability in DMs due to measurable parameters that result in variability of the response

and DM. In particular, temperature measurements have been used in previous research to account for variability due to environmental conditions (Olund, 2004). Thermal changes in bridge structures have been observed to cause changes in the structure's boundary conditions which can lead to changes in the DMs. This study will further explore the variability and correlation of DMs with characteristics of the truck traffic actually passing over the bridge. For example, the weight of the truck or length of the truck may have an influence on the DMs that can be characterized.

One possible approach to account for thermal and truck weight effects on the damage measures that has been applied successfully to other bridges in Connecticut for BHM is the use of conditional distributions of the DMs. The temperature range can be divided into bins where measured events are separated. Further, each temperature bin can also be subdivided into truck weight bins, for example. When a probabilistic BHM method is applied, the distribution of the DM from each temperature and truck weight bin of the baseline time period is compared to that of the same temperature and truck weight bin for the current time period to see if that distribution has varied. A temperature and truck weight dependent p-value, $p_{T_1<T<T_2 \cap W_1<W<W_2}$ can then be determined. The associated temperature and truck weight dependent p-values can be equally weighted and averaged over all of the temperature bins such that

$$\bar{p} = \frac{1}{N}\frac{1}{M}\sum_{n=1}^{N}\sum_{m=1}^{M} p_{\Delta T\cdot(n-1)<T<\Delta T\cdot n \cap \Delta W\cdot(m-1)<W<\Delta W\cdot m} \tag{23}$$

where $\bar{p}$ is the average p-value for all temperatures and truck weights, N is the number of temperature bins, M the number of truck weight bins, ΔT is the size of the temperature bin and ΔW is the size of the truck weight bin. The $\bar{p}$ value is then compared

to a prescribed significance level to determine if the null hypothesis, that the means of the various distributions are equal, can be rejected.

6-CONCLUSION

The prototype BHM/BWIM system including sensors, data acquisition system deployed on the Meriden Bridge, BWIM/BHM methodology, and results of BWIM test were described.

A new BWIM method that provides for non-intrusive means of obtaining weigh-in-motion data is presented and an initial field test was conducted as part of a pilot study where a truck of known-weight conducted multiple passes over the instrumented bridge. Based on this initial field test, the system was calibrated and weigh-in-motion data (i.e. speed, axle-spacing and weight data) were calculated. Foil-type strain sensors are observed to provide better strain measurements during truck crossings than the piezoelectric strain sensors due to a larger time constant. Both accelerometers provide similar measurements above 3 Hz. The calculated speed, axle spacing and weight data are in reasonable agreement with the measured data. Inaccuracies due to multiple vehicle presence on the bridge can be addressed by considering the response of multiple girders. Truck speed measurements, observed to be critical in the accurate calculation of axle spacing and weight, can be enhanced by using accelerometers with larger bandwidth. The second phase of the project will explore these enhancements and validate the BWIM methodology with vehicles from the traffic stream and variations in temperature.

Additionally, BWIM data collected continuously will be validated periodically throughout the project to ensure the system is robust and stable in operation. To evaluate the BHM capabilities of the system, the bridge health monitoring data will be assimilated

into the network of long-term bridge monitoring in Connecticut where the damage measures will be determined and saved to a CTDOT repository for analysis over time.

The proposed BHM method to be used in the dual BHM/BWIM system is described. The components of the BHM method, including DMs, a probabilistic framework, and the mechanism to leverage BWIM data to improve accuracy of BHM, are presented.

REFERENCES

ASTM E1318 Road and Paving Standards, (2009) "Standard Specification for Highway Weigh-In-Motion (WIM) Systems with User Requirements and Test Methods," Designation: E 1318-09.

Bendat, J.S, Piersol, A.G. *Random Data: Analysis and Measurement Procedures*. John Wiley and Sons, Inc., New York, 2000.

Cardini, A.J. and DeWolf, J.T. (2009). "Long-Term Structural Health Monitoring of a Multi-girder Steel Composite Bridge Using Strain Data," submitted for publication.

Cardini, A.J. and DeWolf, J.T. (2009). "Development of a Long-Term Bridge Weigh-In-Motion System for a Steel Girder Bridge in the Interstate Highway System," submitted for publication.

Caicedo, J., Dyke, S.J. and Johnson, E.A. (2000). "Health Monitoring Based on Component Transfer Functions," *Advances in Structural Dynamics,* (Ko, J.M. and Y.L. Xu, eds.) Vol. II, pp. 997-1004.

Chang, F.K. (2000). *Structural Health Monitoring* 2000. Technomic, Lancaster, PA.

Chakraborty, A. and Okaya, D. (1995). "Frequency-Time Decomposition of Seismic Data using Wavelet-Based Methods," *Geophysics*, Vol. 60, No. 6, pp. 1906-1916.

Christenson, R, Bakulski, S., and McDonnell, A. (2011), "Establishment of a Dual-Purpose Bridge Health Monitoring and Weigh-in-Motion System for a Steel Girder Bridge", Transportation Research Board 90th Annual Meeting, Washington, DC
ASTM E1318 Road and Paving Standards, (2009), "Standard Specification for Highway Weigh-In-Motion (WIM) Systems with User Requirements and Test Methods", E 1318-09.

Connecticut Academy of Science and Engineering (2008). "A Study of Weigh Station Technologies and Practices," a report by the Connecticut Academy of Science and Engineering for the Connecticut Department of Transportation, November 2008.

DeWolf, J.T., Cardin, A.J., Olund, J.K. and D'Attilio, P.F. (2009). "Structural Health Monitoring of Three Bridges in Connecticut," Transportation Research Board 88th Annual Meeting, Washington DC, January 11-15, 2009.

Doebling, S.W., Farrar, C. R., Prime, M. B. and Shevitz, D. W. (1996). "Damage Identification and Health Monitoring of Structural and Mechanical Systems from Changes in their Vibration Characteristics: A Literature Review," *Report LA: I3070-MS*, Los Alamos National Laboratory, NM.

Farrar, C.R., Duffy, T.A., Doebling, S.W. and Nix, D.A.. "Vibration-Based Structural Damage Identification," In *Proceedings of the 2nd International Workshop on Structural Health Monitoring*, 2nd International Workshop on Structural Health Monitoring, Stanford, CA, 1999, pp. 764-773.

Farrar, C. R., Baker, W. B., Bell, T. M., Cone, K. M., Dading, T. W., Duffey, T. A., Ekiund, A. and Migliori, A. (1994). "Dynamic Characterization and Damage Detection in the I-40 Bridge over the Rio Grande," *Las Alamos Report LA- 12767-MS UC-906*, June 1994, 15, pp. 3.

Farrar, C. R. and Doebling, S. W. (1997). "Lessons Learned from Applications of Vibration Based Damage Identification Methods to Large Bridge Structure," Structural Health Monitoring: Current Status and Perspectives, 351-370, ed. F. K. Chang, Technomic Pub. Lancaster, PA.

FHWA (Federal Highway Administration) 2001. "Traffic Monitoring Guide," Office of Highway Policy Information, May 1, 2001.

FHWA (Federal Highway Administration) 2005. "Safe, Accountable, Flexible, Efficient Transportation Equity Act: A Legacy for Users, A Summary of Highway Provisions."

Jacob, B. (2002). "Weigh-in-Motion of Axles and Vehicles for Europe," Final Report of the Project WAVE, LCPC, Paris, France.

Moses, F. (1979). "Weigh-in-Motion System using Instrumented Bridges," American Society of Civil Engineers, Transportation Engineering Journal, v 105, n 3, May, 1979, pp. 233-249

McDonnell, A.M. (2000). "Evaluation of Quartz-Piezoelectric WIM Sensors: Second Year Study," NATMEC 2000, August 29, 2000, Madison, WI, 13 pages.

Olund, J.K., Cardini, A.J., D'Attilio, P., Feldblum, E. and DeWolf, J.T. (2006). "Connecticut's Bridge Monitoring Systems," NDE Conference on Civil Engineering, St. Louis, MO, 173-179.

Ojio, T. and Yamada, K. "Bridge Weigh-In-Motion Systems Using Stringers of Plate Girder Bridges," Pre-Proceedings of the Third International Conference on Weigh-In-Motion, (2002): 209-218.

Olund, J. Long Term Structural Health Monitoring of Connecticut's Bridge Infrastructure with a Focus on a Composite Steel Tub-Girder Bridge. M.S. Thesis. The University of Connecticut, 2006.

Scianna, A. and Christenson, R. "Implementation of a Probabilistic Bridge Health Monitoring Network on a Highway Bridge," Fifth New York City Bridge Conference, August 17-18, 2009.

Salawu, O.S. and Williams, C. (1995). "Review of Full-Scale Dynamic Testing of Bridge Structures," Eng. Struc. 17(2): 113-121.

Salawu, O.S. (1997). "Detection of Structural Damage through Changes in Frequency Review," Eng. Struct. 19(9)718-723.

Transportation Research Board, Research in Progress, "Bridge Weigh-in-Motion (B-WIM) System Testing and Evaluation", website http://rip.trb.org/browse/dproject.asp?n=13137, accessed July 23, 2010.

Wall C. and Christenson, R. (2009). "A Bridge Weigh-In-Motion Case Study in Connecticut," to be submitted to the Annual Meeting of Transportation Research Board, Washington D.C.

Connecticut Permanent Long-Term Bridge Monitoring Network, Volume 1: Monitoring of Post-Tensioned Segmental Concrete Box-Girder Bridge - I-95 over the Connecticut River in Old Saybrook (Bridge # 6200). (pdf 1179 kb), Final Report, Adam Scianna, Stephen Prusaczyk, Zhaoshuo Jiang, Richard E. Christenson, John T. DeWolf, CTDOT Report No. CT-2256-2-13-2,August 2014

Connecticut Permanent Long-Term Bridge Monitoring Network Volume 2: Monitoring of Curved Post-Tensioned Concrete Box-Girder Bridge -I-384 WB Over I-84 in East

Hartford (Bridge # 5686) (pdf 785 kb), Final Report, Adam Scianna, Stephen Prusaczyk, Zhaoshuo Jiang, Richard E. Christenson, John T. DeWolf, Jeong-Ho Kim CTDOT Report No. CT-2256-3-13-4,August 2014

Connecticut Permanent Long-Term Bridge Monitoring Network Volume 3: Monitoring of a Multi-Steel Girder Composite Bridge - I-91 SB over the Mattabesset River in Cromwell (Bridge # 3078) (pdf 836 kb), Final Report, Shelly Plude, Stephen Prusaczyk,Adam Scianna, Zhaoshuo Jiang, Richard E. Christenson,Jeong-Ho Kim, John T. DeWolf CTDOT Report No. CT-2256-4-13-5,August 2014

Connecticut Permanent Long-Term Bridge Monitoring Network Volume 4: Monitoring of Curved Steel Box-Girder Composite Bridge- I-84 EB Flyover to I-91 NB in Hartford (Bridge # 5868) (pdf 1031 kb), Final Report, Adam Scianna, Stephen Prusaczyk, Zhaoshuo Jiang, Richard E. Christenson, John T. DeWolf, CTDOT Report No. CT-2256-5-13-6,August 2014

Connecticut Permanent Long-Term Bridge Monitoring Network Volume 5: Wireless Monitoring of the Hung Span in a Large Truss Bridge -I-95 NB over the Thames River in New London (Bridge # 3819) (pdf 912 kb), Final Report, Adam Scianna, Stephen Prusaczyk, Richard E. Christenson, John T. DeWolf, CTDOT Report No. CT-2256-6-13-7,August 2014

Connecticut Permanent Long-Term Bridge Monitoring Network Volume 6 : Monitoring of a Continuous Plate Girder Bridge with Load Restrictions - Route 15 Over the Housatonic River in Stratford (Bridge # 761) (pdf 223 kb), Final Report, Stephen Prusaczyk, Harinee Trivedi, Richard E. Christenson, John T. DeWolf, CTDOT Report No. CT-2256-7-13-8,August 2014

Connecticut Permanent Long-Term Bridge Monitoring Network Volume 7: Lessons Learned for Specifications to Guide Design of Structural Health Monitoring Systems (pdf 3005 kb), Final Report, Richard E. Christenson, John T. DeWolf, Stephen Prusaczyk, CTDOT Report No. CT-2256-8-13-9,August 2014